Electrochemical Determination of Carbendazim in Food Samples Using an Electrochemically Reduced Nitrogen-Doped Graphene Oxide-Modified Glassy Carbon Electrode

Yu Ya[1,2] · Cuiwen Jiang[1,2] · Leixing Mo[1,2] · Tao Li[1,2] · Liping Xie[1,2] · Jie He[1,2] ·
Li Tang[1,2] · Dejiao Ning[1,2] · Feiyan Yan[1,2]

Abstract Nitrogen-doped graphene oxide (NGO) was synthesized via pyrolysis of graphene oxide and urea and was characterized by transmission electron microscopy (TEM) and X-ray photoelectron spectroscopy (XPS). An electrochemically reduced nitrogen-doped graphene oxide-modified glassy carbon electrode (ERNGO/GCE) was developed for the determination of carbendazim (CBZ) in food samples. The surface morphology of the modified electrode was characterized by scanning electron microscopy (SEM). Cyclic voltammetry and electrochemical impedance spectroscopy were employed to demonstrate the large electrode surface and fast electron transfer of the ERNGO/GCE. Electrochemical behaviors of CBZ at different electrodes were studied by voltammetry. Experimental results showed that the ERNGO/GCE achieved better performance for the electrochemical oxidation of CBZ than either the bare glassy carbon electrode (GCE) or the nitrogen-doped graphene oxide-modified GCE (NGO/GCE). Under optimized conditions, the ERNGO/GCE exhibited a wide linearity of 5.0~850 μg/L with a detection limit of 1.0 μg/L (signal-to-noise ratio = 3). Application of our proposed method in food products was shown to be practical and reliable.

Keywords Nitrogen-doped graphene oxide ·
Electrochemically reduced · Carbendazim · Electroanalysis

✉ Feiyan Yan
yanfeiyan2014@126.com

1   Institute for Agricultural Product Quality Safety and Testing Technology, Guangxi Academy of Agricultural Sciences, Nanning 530007, China

2   Quality Inspection and Test Center for Sugarcane and Its Product, China Ministry of Agriculture (Nanning), Nanning 530007, China

Introduction

Carbendazim (CBZ) is a broad-spectrum fungicide. It has been widely used in the prevention and control of various diseases that affect crops, fruits, and vegetables (Devi et al. 2015; Thomidis et al. 2009). Recently, toxicology studies suggested that CBZ can have potentially harmful effect on human health (Farag et al. 2011; Rama et al. 2014). Additionally, CBZ can persist for a long time in the environment, crops, fruits, and vegetables (Lewandowska and Walorczyk 2010). Therefore, developing an accurate, sensitive, and simple method for the determination of CBZ has practical significance for the environment and human health. Different analytical methods had been adopted for CBZ detection, including chromatography (Chen et al. 2015a; Qin et al. 2016; Subhani et al. 2013), spectrophotometry (Chen et al. 2015b; Pourreza et al. 2015; Strickland and Batt 2009), and chemiluminescence (Liao and Xie 2006; Llorent-Martínez et al. 2013). In addition, electroanalytical methods have been used in CBZ detection and have particular advantages such as high sensitivity, ease of operation, short analysis time, and low cost. Many different kinds of materials were used as electrode modifier for CBZ electrochemical detection, owing to the poor response of CBZ at the unmodified electrode. Among these materials, carbon-based nanomaterials are the most commonly used types. A variety of carbon nanotube-based electrochemical sensors, decorated with anionic surfactant (Petroni et al. 2016), mesoporous silica (Razzino et al. 2015), and graphene oxide (Luo et al. 2013), had been fabricated toward electrochemical oxidation of CBZ. We described an advanced electrochemical sensor for the determination of carbendazim based on pyrrolidinium ionic liquid/ordered mesoporous carbon composite system (Ya et al. 2015). Graphene was used as a promising electrode modifier for the fabrication of novel CBZ electrochemical sensor due to its

distinct physical and chemical attributes (Noyrod et al. 2014). Diamond electrode, one of the carbon-based material electrodes, is also a powerful tool for the electroanalysis of CBZ (França et al. 2012; Lima et al. 2016). Meanwhile, other research had presented carbendazim quantification by electrochemical methods using various modified electrodes, such as hetropolyacid montmorillonite clay-modified electrode (Manisankar et al. 2006), carboxylic group functionalized poly (3,4-ethylenedioxythiophene) mimic electrode (Yao et al. 2014), and zeolite-modified electrode (Maximiano et al. 2016).

Graphene is a two-dimensional layer of carbon atoms with an extended honeycomb network and has been the subject of much attention since its first artificial exfoliation in 2004 (Novoselov et al. 2004). It is widely used in electroanalysis because of its extraordinary physical and chemical properties, such as its high surface area, high thermal conductivity, high chemical stability, and rapid charge carrier mobility (Li et al. 2015; Wei et al. 2016). Chemical doping with heteroatoms, such as N, B, or P, can be used to tailor the electronic and chemical properties of graphene (Wang et al. 2014). Among these elements, nitrogen is considered to be an excellent dopant for graphene because of its comparable atomic size and number of valence electrons. Nitrogen doped in graphene can improve the electrical conductivity and stability of graphene and also leads to the formation of an increased activation region on the graphene surface (Usachov et al. 2011). Thus, nitrogen-doped graphene has great potential application in the field of electroanalysis (Shao et al. 2010; Wang et al. 2010).

Graphene is limited in electrochemical applications because of its irreversible agglomeration (Kuila et al. 2012). It is known that graphene oxide has good dispersibility in many solvents because of the polar oxygens that render graphene oxide strongly hydrophilic. However, because of the oxygen-containing groups, the electrical conductivity of the modified interface decreases, and this may limit the direct application of graphene oxide in the field of electroanalysis (Chen et al. 2012). At the same time, oxygen-containing groups of graphene oxide can be reduced, thus restoring a more perfect graphene structure with planar conjugation and further improving the conductivity of graphene oxide (Liu et al. 2014; Qiao et al. 2015). In this work, we describe a sensitive, reliable, and simple electrochemical method for the detection of CBZ based on an electrochemically reduced nitrogen-doped graphene oxide-modified glassy carbon electrode (ERNGO/GCE). It is noted that the oxidation signal of CBZ improves significantly for ERNGO/GCE compared to the nitrogen-doped graphene oxide-modified glassy carbon electrode (NGO/GCE). This is attributed to the large electrically active area and excellent electrical conductivity of the ERNGO/GCE.

Experimental

Reagents and Apparatus

Carbendazim (99.0 %) was obtained from Dr. Ehrenstorfer GmbH Company (Augsburg, Germany). Potassium ferrocyanide and potassium hexacyanoferrate were purchased from Sigma Aldrich (St. Louis, MO, USA). Graphite powder, sodium nitrate, potassium permanganate, sulfuric acid, and hydrogen peroxide were supplied from Sinopharm Chemical Reagent Co., Ltd. (Shanghai, China). All other reagents were of analytical grade and were used as received. A phosphate buffer solution (PBS) was prepared from KOH and 0.1 M H_3PO_4, and the pH was monitored using a pH meter. All aqueous solutions were prepared in deionized water.

Electrochemical experiments were performed on a CHI760E electrochemical workstation (Chenhua Instrument Co. Ltd., China). A conventional three-electrode system was used for all electrochemical experiments. A bare or modified glassy carbon electrode (GCE) of 3 mm diameter was the working electrode, a saturated calomel electrode was used as the reference electrode, and a platinum wire electrode was used as the auxiliary electrode. X-ray photoelectron spectroscopy (XPS) analysis was performed using a VG MultiLab2000 spectrometer (ThermoVG scientific, UK). Transmission electron microscopy (TEM) images were obtained on a Tecnai G2 F20 S-Twin microscope (FEI, USA). The surface morphology of the electrodes was characterized by a S-3400N scanning electron microscope (SEM) (Hitachi Co., Japan). pH values were measured using a pH-3C precision pH meter (Leici Instruments, China).

Preparation of NGO

NGO was prepared according to a previously reported method (Du et al. 2014). In a typical synthesis, 1.0 graphite powder, 0.50 g sodium nitrate, and 50 mL sulfuric acid were mixed in ice-water bath. Nine grams of potassium permanganate was slowly added into the mixture in 2 h. Then, 1.0 g melamine was put into suspension obtained above. After stirring at 30 °C for 12 h, 46 mL hot deionized water was added into the suspension dropwise. This process was performed at 90 °C for 1 h. Subsequently, 20 mL of hydrogen peroxide was added into the suspension. Afterward, 30 min of ultrasonication was taken with the power of 200 W. The resulting suspension was centrifuged at 4000 rmp for 20 min to obtain mud-like material. The obtained material was washed with deionized water and ethanol for several times. Then, the product was dried at 40 °C for 2 days to get NGO.

Preparation of Modified Electrode

The GCE was polished to a mirror-like surface with a 0.05 μm alumina slurry and was ultrasonically washed in a 1:1 nitric acid solution, alcohol, and deionized water for 5 min, respectively. The GCE was then dried with a high-purity nitrogen steam. One milligram of NGO was dispersed in 1.0 mL of ethanol by ultrasonication for 1 h to form a homogenous suspension. Then, 5 μL of the obtained suspension was dipped onto the surface of the GCE and dried at room temperature; the obtained modified electrode was denoted as NGO/GCE. The ERNGO/GCE was fabricated by the following procedure: a cyclic voltammetric scan was run from 0 to −1.0 V with a scan rate of 25 mV/s using NGO/GCE as the working electrode in 0.1 M KNO$_3$ followed by sweeping 20 segments for efficient reduction of NGO.

Analytical Procedure

For the determination of CBZ, the three-electrode system was immersed in 10-mL aliquots of pH 4.0 PBS containing different concentrations of CBZ. After 240 s of accumulation, differential pulse voltammetry (DPV) measurements were recorded from 0.50 to 1.20 V, and the oxidation peak currents at 0.90 V were measured for CBZ with the following parameters: a potential increase of 0.004 V, an amplitude of 0.05 V, a pulse width of 0.05 s, and a pulse interval of 0.5 s.

Results and Discussion

Characterization of NGO

The XPS spectra of NGO are presented in Fig. 1. The wide-scan (Fig. 1a) and high-resolution spectra (Fig. 1b) of NGO reveal the presence of nitrogen in *N*-graphene, indicating that nitrogen was successfully doped into the graphene oxide. Figure 1c shows the TEM images of NGO. The typical wrinkle and flake of the graphene sheet are clearly observed in the image. Such wrinkled structure is highly beneficial in maintaining a high surface area on the electrode since the sheets cannot readily collapse back to a graphitic structure (Du et al. 2011).

Characterization of Modified Electrodes

The surface morphologies of the bare GCE, NGO/GCE, and ERNGO/GCE were characterized by SEM as shown in Fig. 2a, b, c, respectively. As seen in these images, the surface of the bare GCE is smooth and virtually featureless. On the surface of the NGO/GCE, the typical wrinkled feature is slightly visible, indicating that the NGO successfully modified the surface of the GCE. After electrochemical reduction, the wrinkled structure is clearly observed on the surface of the ERNGO/GCE, showing higher surface roughness. This surface structure of the ERNGO/GCE is highly beneficial in maintaining a high surface area on the electrode (Sun and Wang 2015).

Fig. 1 **a** XPS spectra of NGO. **b** High-resolution spectrum of N 1s in NGO. **c** TEM image of NGO
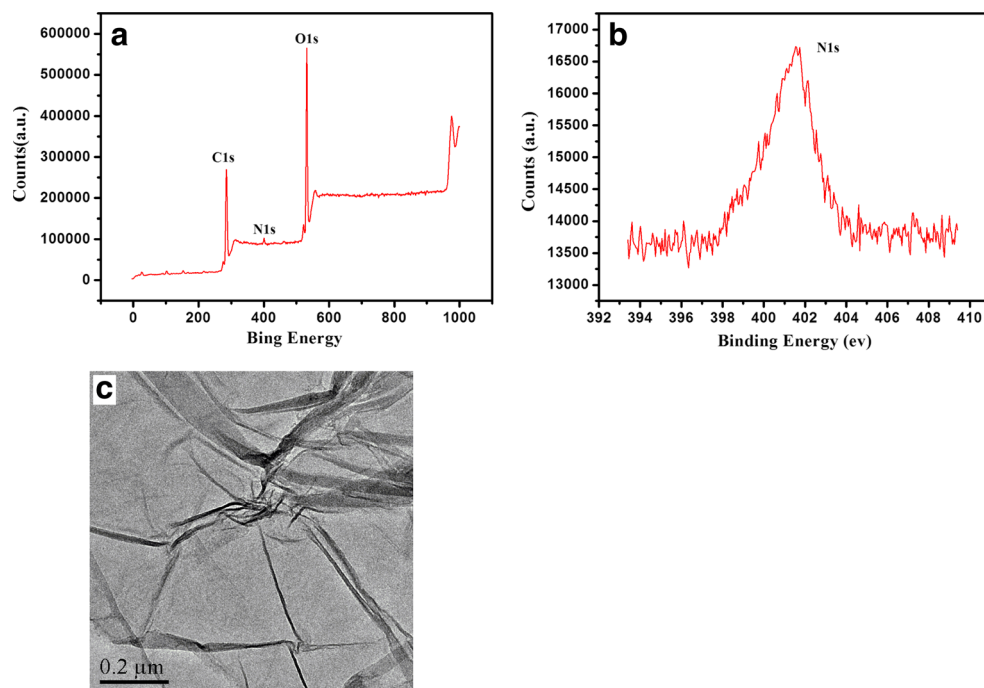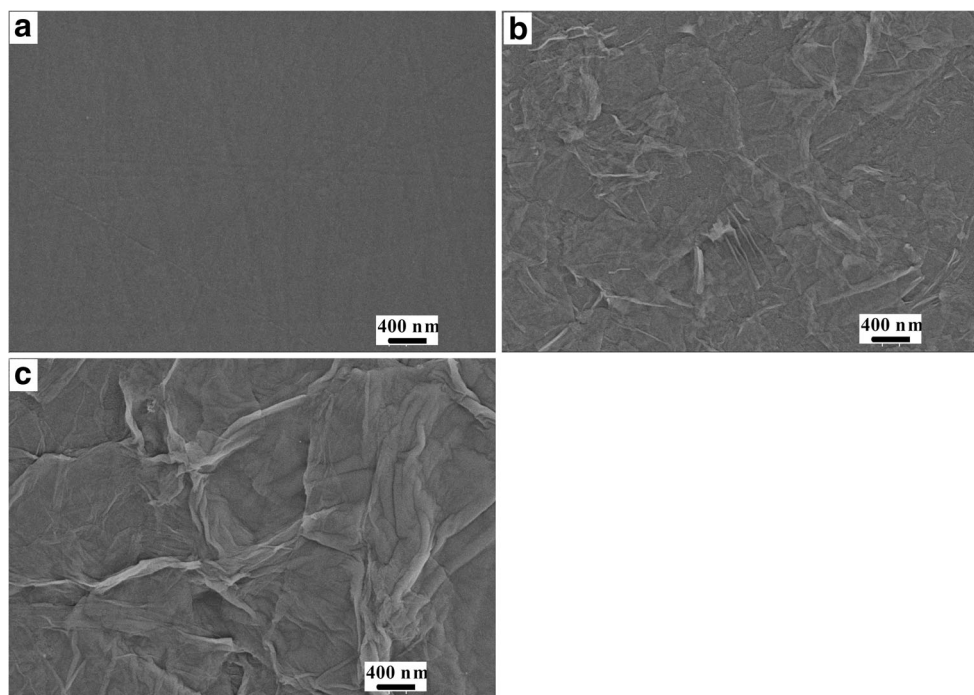
Fig. 2 SEM images of bare GCE (**a**), NGO/GCE (**b**), and ERNGO/ GCE (**c**)


The electrochemical characterizations of the different electrodes in the presence of an external redox probe $[Fe(CN)_6]^{3-/4-}$ were carried out using cyclic voltammetry and electrochemical impedance spectroscopy. Figure 3a shows the cyclic voltammograms of 5.0 mmol/L $[Fe(CN)_6]^{3-/4-}$ for the bare GCE (curve a), the NGO/GCE (curve b), and the ERNGO/ GCE (curve c) at a scan rate of 50 mV/s. A pair of redox peaks for $[Fe(CN)_6]^{3-/4-}$ is shown for the bare GCE with a peak-to-peak separation ($\triangle E_p$) of 167 mV. For the NGO/GCE, both the cathodic and anodic peak currents increased slightly, and the $\triangle E_p$ value decreased to 101 mV, which indicated high electrocatalytic activity of the NGO. While the $\triangle E_p$ exhibited by the ERNGO/GCE was 67 mV, compared to the NGO/ GCE, the redox peak current increased significantly for the ERNGO/GCE. These results demonstrate that the electrochemical reduction can greatly improve the electrical conductivity and electrocatalytic activity of the NGO. The effect of the scan rate was assessed using the Randles-Sevcik formula (Zhou et al. 2013):

$$I_p = 2.69 \times 10^5 D^{1/2} n^{3/2} A v^{1/2} C$$

where I_p refers to the peak current (μA), D is the diffusion coefficient (cm^2 s$^-$), n is the electron-transfer number, A is the electroactive surface area of the electrode (cm^2), v is the scan rate (V/s), and C is the concentration of $[Fe(CN)_6]^{3-/4-}$ (mmol/L). Here, $D = 0.76 \times 10^{-5}$, $n = 1$, $v = 0.050$, and $C = 5.0$. As calculated from this formula, the electroactive areas of the bare GCE, NGO/GCE, and ERNGO/GCE are 0.055, 0.071, and 0.092 cm^2, respectively. These results indicate that the electrochemical reduction of NGO effectively improved the electroactive area of the electrode surface.

Figure 3b shows the spectra from electrochemical impedance spectroscopy represented as Nyquist plots for the bare GCE (curve a), NGO/GCE (curve b), and ERNGO/GCE (curve c) in 5.0 mmol/L $[Fe(CN)_6]^{3-/4-}$. A clear semicircle is observed on the bare GCE and NGO/GCE. However, the ERNGO/GCE exhibits a nearly straight line. The

Fig. 3 Cyclic voltammetry curves (**a**) and Nyquist plots of electrochemical impedance spectroscopy (**b**) of the GCE (*a*), NGO/GCE (*b*), and ERNGO/ GCE (*c*) in 5.0 mmol/L $[Fe(CN)_6]^{3-/4-}$
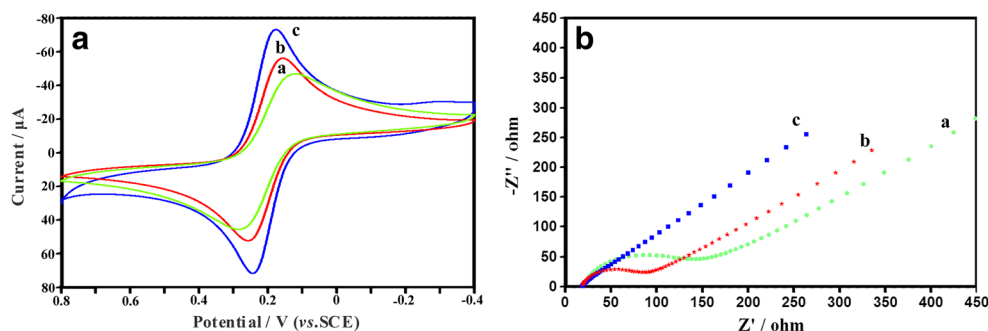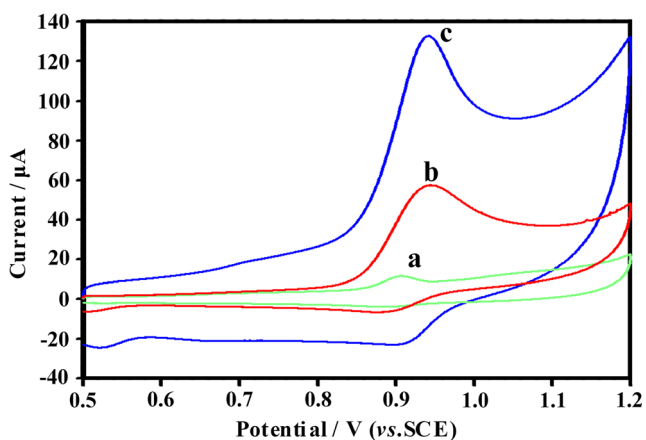
Fig. 4 Cyclic voltammetry curves for 300 μg/L CBZ in pH 4.0 PBS at the GCE (*a*), NGO/GCE (*b*), and ERNGO/GCE (*c*)

electrochemical impedance spectroscopy result confirms that electrochemical reduction can further improve the conductivity of NGO.

Electrochemical Behaviors of CBZ at Different Electrodes

Electrochemical behaviors of CBZ at different electrodes were investigated with cyclic voltammograms, and these are shown in Fig. 4. As illustrated in Fig. 4, a very weak anodic peak was found for the bare GCE (curve a). In contrast, a well-defined anodic peak with significantly increasing peak current was observed for the NGO/GCE (curve b), indicating that NGO has remarkable enhancing effects on the electrochemical oxidation of CBZ. At the same time, a sharp anodic peak can be seen for the ERNGO/GCE (curve c). The peak current of CBZ for the ERNGO/GCE was onefold higher than that for the NGO/GCE (curve b). This result may be attributed to two factors: (1) ERNGO provides a larger electroactive area which increases the loading amount of CBZ at the modified electrode surface and (2) the excellent conductivity of ERNGO can

accelerate electron transfer between the modified electrode and CBZ in solution.

Effect of Scan Rate

The linear sweep voltammetry technique was used to probe the effect of the scan rate on the electrochemical oxidation of CBZ. Figure 5a shows the relationships between the scan rate and the current responses for 150 μg/L of CBZ at the ERNGO/GCE. The current response increased linearly with the scan rate in the range of 25~200 mV/s and can be expressed as the following: I_p (μA) = 0.03406 v (mV/s) + 1.977(r = 0.997). This finding indicates that the electrochemical oxidation of CBZ at the ERNGO/GCE is an adsorption-controlled process. In addition, a linear relationship between the oxidation peak potential (E_{pa}) and Napierian logarithm of scan rate (ln v) is also observed in the scan rate range of 25~200 mV/s (Fig. 5b). A linear calibration curve with a regression equation of E_{pa} (V) = 0.9980 + 0.02477 ln v (V/s) (r = 0.996) was obtained. For an adsorption-controlled and totally irreversible electrode process, the relationship between E_{pa} and ln v is expressed through the Laviron's equation (Laviron 1974):

$$E_{pa} = E^0 + \frac{RT}{[anF]} \ln \left[\frac{RTk}{anF} \right] + \left[\frac{RT}{anF} \right] \ln v$$

where E_{pa} is the oxidation peak potential (V), E^0 is the formal potential, R is the universal gas constant (8.314 J/mol K), T is the temperature (298 k), α is the electron-transfer coefficient, n is the electron-transfer number, F is the Faraday constant (96,480 C/mol), and v is the scan rate (V/s). In our study, αn is calculated to be 1.0367. Usually, α is assumed as 0.5 in a totally irreversible electrode process. The obtained for n is 2.07 ≈ 2.0. So, two electrons are involved in the electrochemical oxidation of CBZ.

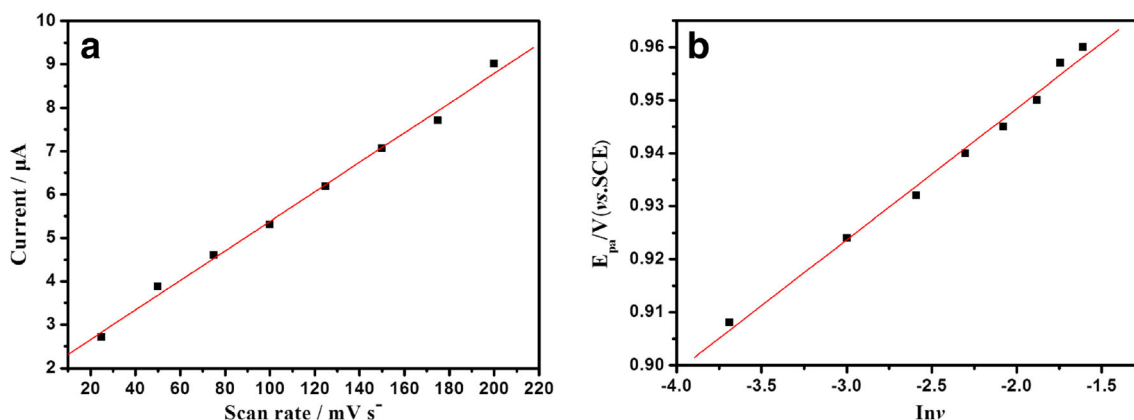**Fig. 5** **a** The relationship between the current response for 150 μg/L CBZ at the ERNGO/GCE in pH 4.0 PBS and the scan rate. **b** The plot of oxidation peak potential of CBZ versus Napierian logarithm of scan rate
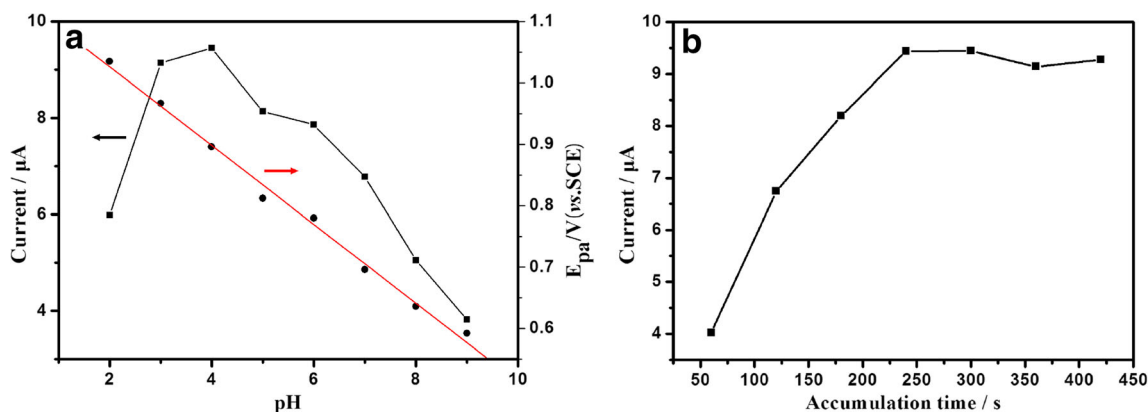
Fig. 6 **a** Effect of pH on peak current and E_{pa} of 300 μg/L CBZ at the ERNGO/GCE. **b** The effect of accumulation time on the peak current for 300 μg/L CBZ at the ERNGO/GCE

Effect of pH and Accumulation Time

The influence of pH on the current response for 300 μg/L of CBZ at the ERNGO/GCE was investigated in the pH range from 2.0 to 9.0 using DPV (Fig. 6a). The results indicate that solution pH influences the oxidation peak current of CBZ. The peak current increased with decreasing pH in the range of 9.0 to 4.0 and decreased at lower pH values. Thus, a pH value of 4.0 was adopted for subsequent analytical experiments. The relationship between E_{pa} and pH was also depicted in Fig. 6a. As we can see, E_{pa} linearly shifted negatively with the increasing of pH value, which suggested that protons participated in the electrochemical oxidation of CBZ directly. A good linear relationship between E_{pa} and pH was constructed with a linear regression equation expressed as $E_{pa} = 1.15{-}0.064$ pH ($r = 0.997$). The slope value of −64 mV/pH was close to the theoretical value of −59 mV/pH, indicating that the number of electron transfer was equal to the proton number involved in the electrochemical oxidation of CBZ. Thus, the electrochemical oxidation of CBZ involves two electrons and two protons, which is in agreement with the literature reported. (Yao et al. 2014). The electrochemical oxidation of CBZ can be elucidated in Scheme 1.

The influence of accumulation time on current responses of CBZ was investigated in the range of 60 to 360 s (Fig. 6b). Peak currents increased rapidly up to240 s and changed slightly when accumulation time was longer than 240 s. Therefore, an accumulation time of 240 s was chosen for all of the experiments.

Analytical Performance of ERNGO/GCE

Under the optimized conditions, DPV was used to electrochemically determine CBZ on the ERNGO/GCE. Figure 7 gives the DPV responses at different concentrations of CBZ. It is clear that, with an increase in CBZ concentration, the current response increased gradually. The current response showed good linear correlation with CBZ concentration from 5.0 to 850 μg/L. The regression equation for this relationship was I_p (μA) $= 0.02258C$ (μg/L) $+ 0.5972$ ($r = 0.997$). The detection limit was calculated as 1.0 μg/L (signal-to-noise ratio = 3).

Reproducibility and Stability

The reproducibility of the ERNGO/GCE was evaluated by repeated measurement of 150 μg/L of CBZ. Six different modified electrodes showed a relative standard deviation (RSD) of 5.4 %, and for one electrode, the RSD was 4.2 % for six repeated measurements. The stability of the ERNGO/GCE was investigated after long-term storage in a refrigerator at 4 °C for 1 month, and 90.1 % of the original oxidation peak current was retained. These results indicate that the fabricated modified electrode had good reproducibility and stability.

Interference Study

The selectivity of the ERNGO/GCE was investigated by determination of 100 μg/L of CBZ in the presence of different common interferences. In this study, the tolerance limit was defined as the molar ratio of potential interferences/CBZ that
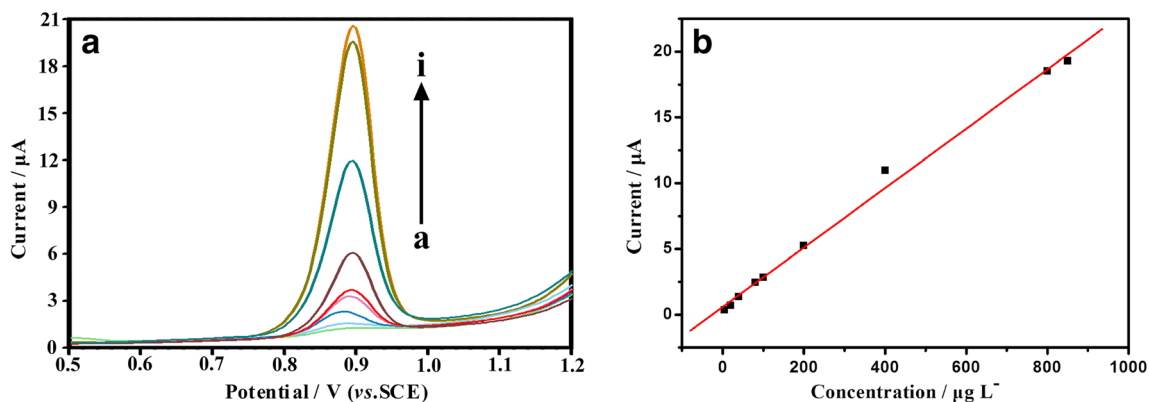
Scheme 1 Electrochemical oxidation of CBZ
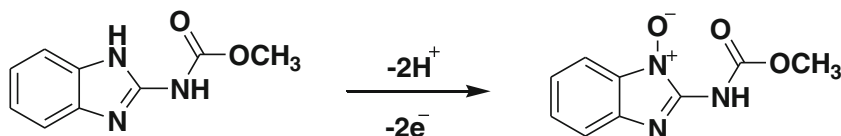
Fig. 7 **a** DPV curves of CBZ at the ERNGO/GCE in pH 4.0 PBS with different concentrations (from *a* to *i*: 5.0, 20, 40, 80, 100, 200, 400, 800, and 850 μg/L, respectively). **b** Linear relationship between the current response and the CBZ concentration

caused the ±5.0 % change in the current response of CBZ. The results revealed that more than 5000-fold sucrose, glucose, and fructose;1000-fold Na^+, K^+, Ca^{2+}, Mg^{2+}, Cu^{2+}, Zn^{2+}, Fe^{3+}, Al^{3+}, Cl^-, NO_3^-, CO_3^{2-}, and SO_4^{2-}; and 200-fold methyl parathion, ethyl parathion, vitamin B_1, B_2, C, and E, L-aspartic acid, glutamic acid, serine, thiophanate, thiophanate-methyl, thiabendazole, endodsulfan, ametryn, fenamiphos, and benomyl did not interfere with the determination of CBZ. As shown in Fig. 8, the peak current of 100 μg/L CBZ at the ERNGO/GCE in the absence (curve a) and presence (curve b) of pesticide mixtures containing 200-fold of methyl parathion, ethyl parathion, thiophanate, thiophanate-methyl, thiabendazole, endodsulfan, ametryn, fenamiphos, and benomyl was about the same. The result suggests that the ERNGO/GCE has good selectivity.

Practical Applications

To evaluate the feasibility of the developed method, the ERNGO/GCE was used to measure the concentration of CBZ in *Dendrobium candidum* samples by using a standard
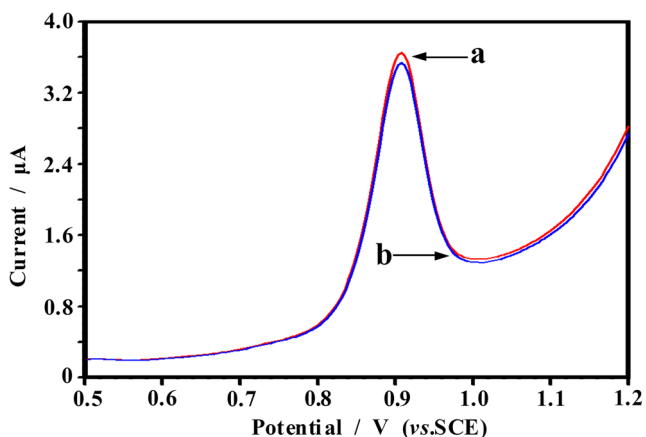

Fig. 8 DPV curves of 100 μg/L CBZ at the ERNGO/GCE in the absence (*a*) and presence (*b*) of pesticide mixtures

addition method. One gram of *D. candidum* power was added to 20 mL of ethanol, and the mixture was sonicated for 5 h. The mixture was then separated by centrifugation at 4000 rpm for 5 min. The resulting ethanol solution was evaporated to dryness using a mild nitrogen stream, and the residue was reconstituted in 1.0 mL of ethanol. One hundred microliters of this ethanol solution was injected into10 mL of pH 4.0 PBS, and then the measurement was made by the method described above. The results are shown in Table 1, and it can be seen that the results were satisfactory. Recovery was in the range of 90.5~94.8 %, indicating that the described method is adequate for practical application in detecting CBZ in real samples.

Conclusions

NGO was successfully synthesized by a simple method and was used as a modifier to the GCE. A novel electrochemical method for the determination of CBZ was developed based on the ERNGO/GCE. As an advanced sensor electrode, the ERNGO/GCE exhibited better electrochemical performance than both the bare GCE and NGO/GCE. This was attributed to the large electroactive area and its good conductivity. The ERNGO/GCE has the advantages of a simple preparation, an easily renewable surface, and a low cost. It is thus expected to have further applications in the electroanalytical field.

Table 1 Results for the determination of CBZ in *Dendrobium candidum* samples

Original (μg/L)	Added (μg/L)	Found (μg/L)	Recovery (%)
0.0	20.0	18.1	90.5
	50.0	47.6	95.2
	100	97.3	97.3
	400	379	94.8

References

Chen D, Feng H, Li J (2012) Graphene oxide: preparation, functionalization, and electrochemical applications. Chem Rev 112:6027–6053

Chen H et al (2015a) Determination of thiophanate-methyl and carbendazim in rapeseed by solid–phase extraction and ultra–high performance chromatography with photodiode array detection. Instrum Sci Technol 43:511–523

Chen M, Zhao Z, Lan X, Chen Y, Zhang L, Ji R, Wang L (2015b) Determination of carbendazim and metiram pesticides residues in reapeseed and peanut oils by fluorescence spectrophotometry. Measurement 73:313–317

Devi PA, Paramasivam M, Prakasam V (2015) Degradation pattern and risk assessment of carbendazim and mancozeb in mango fruits. Environ Monit Assess 187:4142

Du H, Ye J, Zhang J, Huang X, Yu C (2011) A voltammetric sensor based on graphene-modified electrode for simultaneous determination of catechol and hydroquinone. J Electroanal Chem 650:209–213

Du M, Sun J, Chang J, Yang F, Shi L, Gao L (2014) Synthesis of nitrogen-doped reduced graphene oxide directly from nitrogen-doped graphene oxide as a high-performance lithium ion battery anode. RSC Adv 4:42412–42417

Farag A, Ebrahim H, Elmazoudy R, Kadous E (2011) Developmental toxicity of fungicide carbendazim in female mice. Birth Defects Res Part B 92:122–130

França RF, Oliveira HPMD, Pedrosa VA, Codognoto L (2012) Electroanalytical determination of carbendazim and fenamiphos in natural waters using a diamond electrode. Diam Relat Mater 27–28:54–59

Kuila T, Bose S, Mishra AK, Khanra P, Kim NH, Lee JH (2012) Chemical functionalization of graphene and its applications. Prog Mater Sci 57:1061–1110

Laviron E (1974) Adsorption, autoinhibition and autocatalysis in polarography and in linear potential sweep voltammetry. J Electroanal Chem 52:355–393

Lewandowska A, Walorczyk S (2010) Carbendazim residues in the soil and their bioavailability to plants in four successive harvests. Pol J Environ Stud 19:757–761

Li F, Gan S, Han D, Niu L (2015) Graphene-based nanohybrids for advanced electrochemical sensing. Electroanal 27:2098–2115

Liao S, Xie Z (2006) Flow-injection chemiluminescence study of luminal-hydrogen peroxide-carbendazim system. Spectrosc Lett 39:473–485

Lima T, Silva HTD, Labuto G, Simões FR, Codognoto L (2016) An experimental design for simultaneous determination of carbendazim and fenamiphos by electrochemical method. Electroanal 28:817–822

Liu L, Gou Y, Gao X, Zhang P, Chen W, Feng S, Hu F, Li Y (2014) Electrochemically reduced graphene oxide-based electrochemical sensor for the sensitive determination of ferulic acid in A. sinensis and biological samples. Mat Sci Eng C 42:227–223

Llorent-Martínez EJ, Alcántara-Durán J, Ruiz-Medina A, Ortega-Barrales P (2013) Determination of carbendazim in food products using a sequential injection analysis optosensor. Food Anal Methods 6:1278–1283

Luo S, Wu Y, Gou H (2013) A voltammetric sensor based on GO–MWNTs hybrid nanomaterial-modified electrode for determination of carbendazim in soil and water samples. Ionics 19:673–680

Manisankar P, Selvanathan G, Vedhi C (2006) Determination of pesticides using heteropolyacid montmorillonite clay-modified electrode with surfactant. Talanta 68:686–692

Maximiano EM, Lima F, Cardoso CAL, Arruda GJ (2016) Incorporation of thermally activated zeolite into carbon paste electrodes for voltammetric detection of carbendazim traces in milk samples. J Appl Electrochem 46:713–723

Novoselov KS, Geim AK, Morozov SV, Jiang D, Zhang Y, Dubonos SV, Grigorieva IV, Firsov A (2004) Electric field effect in atomically thin carbon films. Science 306:666–669

Noyrod P, Chailapakul O, Wonsawat W, Chuanuwatanakul S (2014) The simultaneous determination of isoproturon and carbendazim pesticides by single drop analysis using a graphene-based electrochemical sensor. J Electroanal Chem 719:54–59

Petroni JM, Lucca BG, Fogliato DK, Ferreira VS (2016) Sensitive approach for voltammetric determination of carbendazim based on the use of an anionic surfactant. Electroanal 28:1362–1369

Pourreza N, Rastegarzadeh S, Larki A (2015) Determination of fungicide carbendazim in water and soil samples using dispersive liquid-liquid microextraction and microvolume UV–vis spectrophotometry. Talanta 134:24–29

Qiao W, Li Y, Wang L, Li G, Li J, Ye B (2015) Electrochemical behavior of daphnetin and its sensitive determination based on electrochemically reduced graphene oxide modified electrode. J Electroanal Chem 749:68–74

Qin X, Xu Y, Sun Y, Zhao L, Wang L, Sun Y, Liang X (2016) Determination of carbendazim and diethofencarb in cotton and soil by high-performance liquid chromatography. Anal Lett 49:1631–1639

Rama EM, Bortolan S, Vieira ML, Moreira EG (2014) Reproductive and possible hormonal effects of carbendazim. Regul Toxicol Pharmacol 69:476–486

Razzino CA, Sgobbi LF, Canevari TC, Cancino J, Machado SAS (2015) Sensitive determination of carbendazim in orange juice by electrode modified with hybrid material. Food Chem 170:360–365

Shao Y et al (2010) Nitrogen-doped graphene and its electrochemical applications. J Mater Chem 20:7491–7496

Strickland AD, Batt CA (2009) Detection of carbendazim by surface-enhanced raman scattering using cyclodextrin inclusion complexes on gold nanorods. Anal Chem 81:2895–2903

Subhani Q, Huang ZP, Zhu ZY, Zhu Y (2013) Simultaneous determination of imidacloprid and carbendazim in water samples by ion chromatography with fluorescence detector and post-column photochemical reactor. Talanta 116:127–132

Sun D, Wang S (2015) Highly sensitive electrochemical sensor for paeonol using NMP-exfoliated grapheme-modified electrode. Ionics 21:1–6

Thomidis T, Michailides T, Exadaktylou E (2009) Contribution of pathogens to peach fruit rot in northern Greece and their sensitivity to iprodione, carbendazim, thiophanate-methyl and tebuconazole fungicides. J Phytopathol 157:194–200

Usachov D et al (2011) Nitrogen-doped graphene: efficient growth, structure, and electronic properties. Nano Lett 11:5401–5407

Wang X, Sun G, Routh P, Kim DH, Huang W, Chen P (2014) Heteroatom-doped graphene materials: syntheses, properties and applications. Chem Soc Rev 43:7067–7098

Wang Y, Shao Y, Matson DW, Li J, Lin Y (2010) Nitrogen-doped graphene and its application in electrochemical biosensing. ACS Nano 4:1790–1798

Wei T, Dai Z, Lin Y, Du D (2016) Electrochemical immunoassays based on graphene: a review. Electroanal 28:4–12

Ya Y, Wang T, Xie L, Zhu J, Tang L, Ning D, Yan F (2015) Highly sensitive electrochemical sensor based on pyrrolidinium ionic liquid modified ordered mesoporous carbon paste electrode for determination of carbendazim. Anal Methods 7:1493–1498

Yao Y, Wen Y, Zhang L, Wang Z, Zhang H, Xu J (2014) Electrochemical recognition and trace-level detection of bactericide carbendazim using carboxylic group functionalized poly (3,4-ethylenedioxythiophene) mimic electrode. Anal Chim Acta 831: 38–49

Zhou N, Li JH, Chen H, Liao CY, Chen LX (2013) A functional grapheneoxide-ionic liquid composites–gold nanoparticle sensing platform for ultrasensitive electrochemical detection of Hg^{2+}. Analyst 138:1091–1097